# Test of the Weak-Equivalence Principle in an Einstein Elevator (*).

E. C. Lorenzini (1), I. I. Shapiro (1), F. Fuligni (2), V. Iafolla (2), M. L. Cosmo (1) M. D. Grossi (1), P. N. Cheimets (1) and J. B. Zielinski (3)

(1) *Harvard-Smithsonian Center for Astrophysics (CfA) - Cambridge, MA, USA*
(2) *Istituto di Fisica dello Spazio Interplanetario (IFSI) - Frascati, Italy*
(3) *Space Research Centre (SRC) - Warsaw, Poland*

(ricevuto l'1 Agosto 1994; revisionato il 22 Agosto 1994; approvato l'8 Settembre 1994)

**Summary.** — A technique for testing the weak-equivalence principle is presented. This technique involves the measurement of differential accelerations between two test masses of different materials (*e.g.*, aluminum and gold) free falling inside a 3 m long cryostat dropped from a 40 km altitude balloon. The free-fall duration is 30 s for a non-propelled cryostat. The falling test masses are part of a high-sensitivity differential detector with a foreseeable sensitivity in detecting differential accelerations of about $1.5 \cdot 10^{-13}\, g/\sqrt{\text{Hz}}$ (at the liquid-nitrogen temperature of 77 K) and $1.5 \cdot 10^{-14}\, g/\sqrt{\text{Hz}}$ (at the liquid-helium temperature of 4 K). The detector is spun about a horizontal axis at a frequency of typically 1 Hz in order to modulate the gravity signal during free fall. The estimated accuracies, with 95% confidence level, in testing the weak-equivalence principle in a 30 s integration time are 5 parts in $10^{14}$ at the temperature of liquid nitrogen and 5 parts in $10^{15}$ at the temperature of liquid helium.

PACS 04.80 – Experimental tests of general relativity and observation of gravitational radiation.
PACS 07.10 – Mechanical instruments and measurement methods.
PACS 06.30 – Measurement of basic quantities.

## 1. – Introduction.

The achievable accuracies of ground-based tests of the weak-equivalence principle (WEP) with laboratory test masses are limited by the Earth's seismic noise and the small strength of a suitable signal source. In his null experiment with a vertical torsion balance, at the turn of the last century, Eötvös used, as the signal source, the component of the Earth's gravity along the local horizontal, which is compensated by an equivalent component of the Earth's centrifugal force. At a latitude of 45° this

(*) Paper presented at the Second William Fairbank Conference on Relativistic Gravitational Experiments in Space and Related Theoretical Topics, Hong Kong, December 13-16, 1993.

gravity component is at its maximum and is equal to $1.7 \cdot 10^{-3}\, g$ (almost three orders of magnitude smaller than the Earth's gravity). The test masses of the torsion balance were pairs of different materials like copper-platinum, copper-asbestos, copper-water, snakewood-platinum and others. Eötvös established the equivalence of gravitational and inertial mass to an accuracy of about 5 parts in $10^8$ [1], later improved to 3 parts in $10^8$ [2].

In their 1962 experiment, Dicke *et al.* also resorted to a vertical-torsion balance with aluminum and gold test masses, but used the gravity attraction of the Sun balanced by the centrifugal force of the Earth in its motion around the Sun (this technique had been first attempted by Eötvös). The strength of this signal source is $6 \cdot 10^{-4}\, g$ (more than three orders of magnitude smaller than the Earth's gravity). Even though the strength of this source is about threefold smaller than that of the Earth's horizontal gravity component, it has the significant advantage of being modulated by the Earth's rotation. This modulation enabled Dicke *et al.* to improve the accuracy in testing the equivalence principle to about 3 parts in $10^{11}$ for the aluminum-gold pair [3].

A similar type of experiment with a torsion-balance, carried out at Moscow State University [4], yielded a stated accuracy of about 1 part in $10^{12}$ for the aluminum-platinum pair.

An alternative technique for testing the equivalence principle makes use of heavenly bodies. Accurate laser ranging from the Earth to optical retroreflectors on the Moon has allowed a very accurate measurement of the Sun's differential attraction of the siliceous Moon and the ferrous Earth and, consequently, has set an upper limit on any possible violation of the principle of equivalence for such materials of 7 parts in $10^{12}$ [5, 6], later improved to 3 parts in $10^{12}$ [7].

Unlike for the torsion balance experiments, the accuracy of lunar laser ranging is not limited by the Earth's seismic noise but rather by the signal strength. Moreover, thanks to the masses of the Moon and the Earth, lunar laser ranging also tests the effect of the gravitational binding energy upon the universality of free fall. For meter-sized laboratory test masses, the gravitational binding energy is only about $10^{-23}$ of the total energy and, consequently, its effect is far too small to be detected with a torsion balance experiment.

## 2. – General description of proposed experiment.

Both isolation from external noise sources and increase of signal strength are essential ingredients for improving the experimental accuracy in testing the equivalence principle with laboratory test masses on Earth. By performing the experiment in free fall rather than in a ground-based laboratory, we can make the signal source equal or comparable to the full Earth's gravity and, with state-of-the-art isolation, we can reduce the external acceleration noise to about 1 pico-$g$.

An orbital free fall, with a drag-free satellite, is advocated for the *Satellite Test of the Equivalence Principle* (STEP) to attain an accuracy of 1 part in $10^{17}$ [8] in testing this principle. Since STEP is not scheduled to fly before the first years of the next millenium, tests of the equivalence principle at intermediate

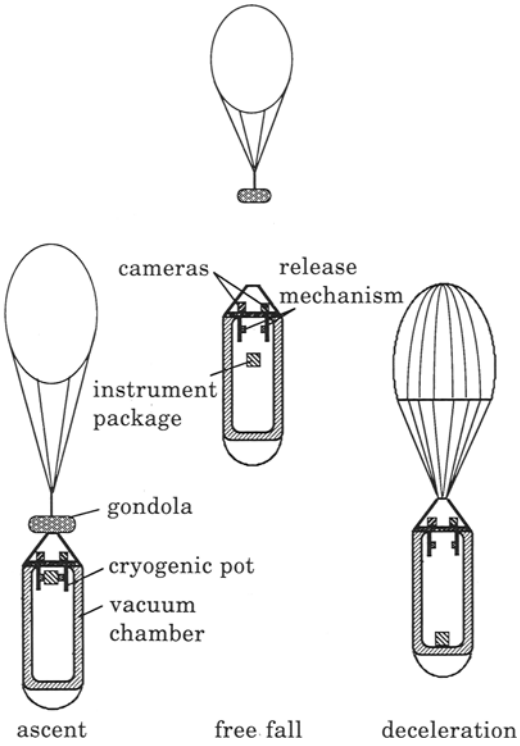


Fig. 1. – Sketch of balloon-released free-fall facility.

accuracy (*i.e.* between $10^{-12}$ and $10^{-17}$) could and probably should be carried out before such a space mission takes place.

We propose the vertical free fall of a very sensitive differential accelerometer inside a 3 m long, evacuated cryostat dropped from a balloon at an altitude of 40 km as an intermediate-accuracy test. The estimated accuracy in testing the weak-equivalence principle with this method is 5 parts in $10^{14}$ at the liquid-nitrogen ($LN_2$) temperature of 77 K and 5 parts in $10^{15}$ at the liquid-helium (LHe) temperature of 4 K as explained later on in this paper.

Under our proposal, the instrument package, which includes the differential acceleration detector, free falls inside a shielding cryostat (see fig. 1). The cryostat is slightly decelerated by the rarefied atmosphere. The instrument package can free fall for 30 s inside the cryostat (see fig. 2) before the detector falls with respect to the cryostat the 3 m distance corresponding to the height of the cryostat; if, however, the cryostat is propelled to compensate for the air-drag deceleration, this time interval can be extended to about 60 s [9-12]. Once the instrument package reaches the cryostat's floor, the cryostat is decelerated by a parachute for retrieval and reflight.

Liquid-nitrogen or liquid-helium refrigeration is adopted to provide low thermal noise, high thermal stability, low thermal gradients, and high $Q$-factors of the acceleration detector. In addition, the acceleration noise of the free-falling instrument package is estimated to be less than $10^{-12} g$ for a pressure inside

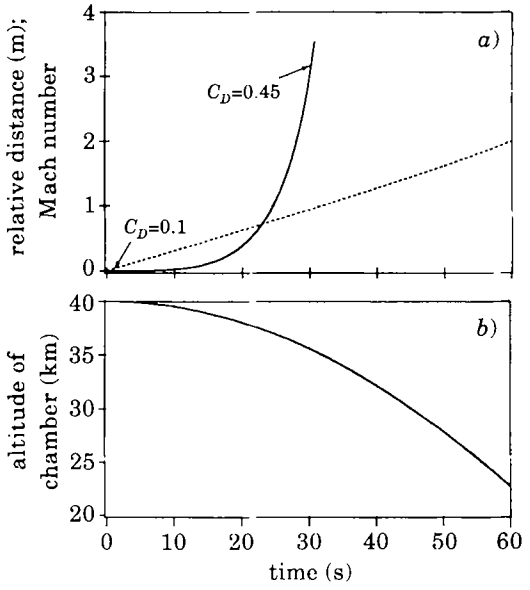


Fig. 2. – Free-fall duration for a non-propelled vacuum chamber. *a*) —— relative distance, --- Mach number; *b*) altitude of chamber.

the cryostat of $10^{-6}$ mbar. These are necessary conditions to achieve the desired differential measurement accuracy.

Consequently, this technique provides free-fall conditions which are unmatched by any other Earth-based drop facility. Presently, available ground-based drop towers provide at most a free-fall time of 5 s and an acceleration noise of at least $10^{-5}g$. Airplanes on parabolic trajectories can fall semi-freely for about 20 s with an acceleration of about $10^{-2}$–$10^{-3}g$. Sounding rockets provide a free-fall time of $\sim 5$ minutes and an acceleration noise around $10^{-4}g$ [13].

## 3. – Description of experimental apparatus.

The gravity detector that we envision is a zero-baseline, differential accelerometer that is based on a technology pioneered by Fuligni and Iafolla for building condenser-type differential force sensors [14-16].

The detector (see fig. 3) measures the differential capacitance, and, consequently, the relative displacement along the sensitive axis $x$, between two double-faced condensers: condenser probe 1 is formed by sensing mass 1 and fixed plates A's and B's; condenser probe 2 is formed by sensing mass 2 and fixed plates C's and D's. The fixed plates A's and C's are used for signal pick-up while the fixed plates B's and D's are for feedback control. The displacement of sensing mass 1, for example, is detected by the series capacitors $A$ and $A'$ which form one branch of a bridge circuit, while two additional reference capacitors form the other branch. The bridge is pumped at a stable frequency of typically 20 kHz in order to keep the noise temperature of the preamplifier at a minimum value. After taking the difference between the output

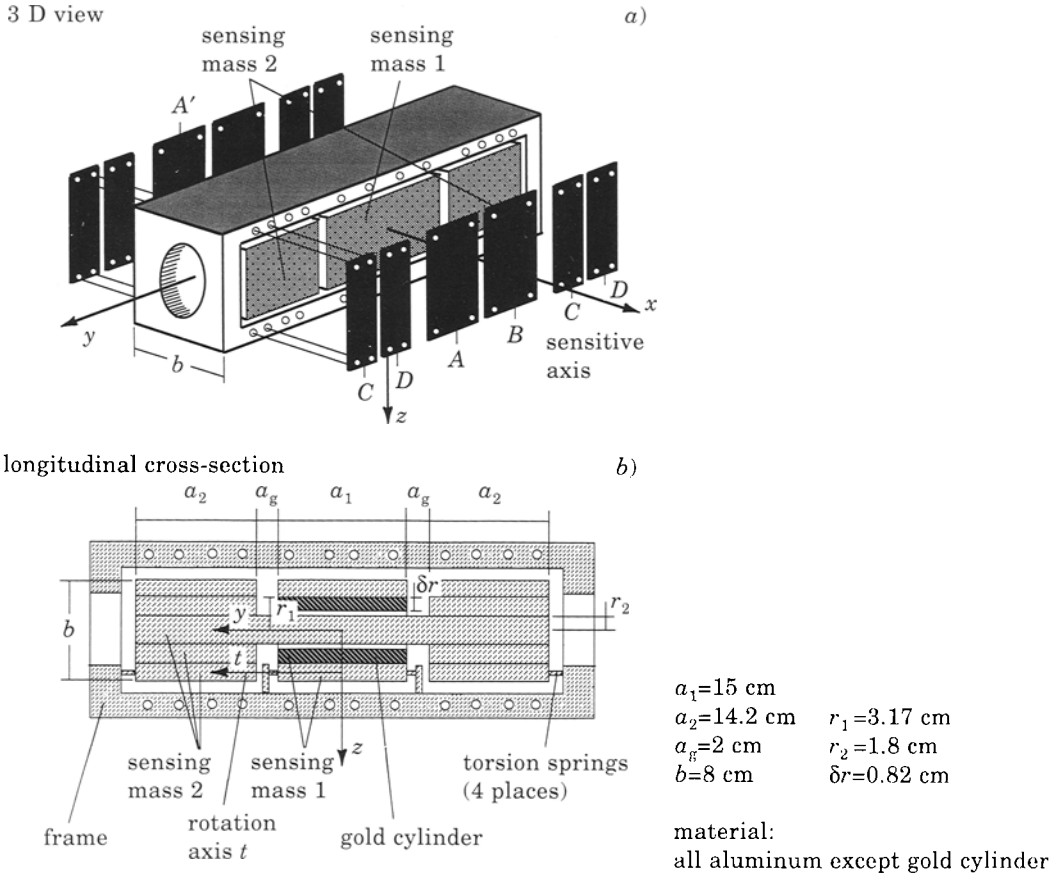


Fig. 3. – Sketch of differential accelerometer.

signals from the condenser probes 1 and 2, the differential output signal is amplified by a low-noise preamplifier, sent to a lock-in amplifier for phase detection and eventually to a low-pass filter.

Figure 3 is a sketch of a possible detector design. The geometry of this particular detector is based on the design of an accelerometer prototype that has already been built. The final design of the detector, however, would likely be modified substantially during a detailed feasibility study. In this particular design, the two sensing masses have prismatic shapes with square cross-sections in order to reduce the gravity gradient torques. Moreover, their centers of mass coincide within less than 4 μm in order to reduce the effect of gravity gradient forces and rotational motion upon the differential output signal. The effects of higher mass moments generated by nearby masses still require a more thorough evaluation which may lead to modifications of the detector's geometry.

Although the selection of materials most suitable for the instrument is still in progress, we will assume in this paper that sensing mass 1 is made entirely of aluminum, while sensing mass 2 consists of a hollow gold cylinder embedded in an aluminum prism. The two sensing masses are constrained by torsional springs to rotate about the $t$-axis (see fig. 3), and their resonant frequencies are electrostatically

controlled for frequency matching. The typical value of the resonant frequency is about 10 Hz. The feedback plates of each condenser probe are used for frequency tuning and for damping the transient oscillations that follow the spin-up and release of the detector.

We obtain gravity signal modulation during free fall by spinning the detector around the horizontal, *i.e.* the $y$-axis (see fig. 3), at a frequency of typically 1 Hz before the release of the instrument into the cryostat. Spinning also provides a frequency separation between the gravity signal and the gravity-gradient–induced accelerations at twice the spin frequency.

Abatement of transient oscillations is provided by electrostatic feedback control of the sensing masses whereby the $Q$-factor is reduced to a value of about five from a value of about 15000 for the test at 77 K and 150000 for the test at 4 K. Consequently, an estimated 2.4 s is required to abate the transient response. When a propelled cryostat is utilized, 30 s of the free-fall duration could be collocated for abating the transient oscillations, thereby easing the demands on the damping process, or nearly the full time could be used, thus doubling the integration time and thereby improving the measurement accuracy by a factor of $\sqrt{2}$.

## 4. – System overview.

The experimental hardware is divided into four major subsystems: 1) gondola; 2) crash frame; 3) cryostat; and 4) instrument package.

1) *Gondola.*

The gondola consists of the components that remain attached to the balloon after the payload has been dropped. Some of these components provide general housekeeping functions; others isolate the payload from balloon rotations. A telemetry system flies with the gondola and permits communication with the ground.

2) *Crash frame.*

The crash frame surrounds the cryostat and instrument package and serves two purposes. First it protects the hardware from damage at impact with the Earth, most likely a water surface. Second it acts as the payload superstructure.

The crash frame, an aluminum tube structure covered with thin fiberglass sheets to reduce air drag, is the only explicit crash protection. Components are loosely connected to the frame through shock absorbers that further limit maximum accelerations.

The crash frame supports the experimental hardware, the telemetry link, and the recovery system, in this case a parachute. The telemetry link broadcasts the status of the equipment and the accelerometer data to the ground station from a small antenna in the noise cone. Attitude stabilization comes from the 2 m long fins on the top of the frame which provide enough return torque during the fall to keep the playload within 5° off vertical. The parachute system is located in the tail section. The peripheral electronics, video cameras, and batteries are also carried in the crash frame.

3) *Cryostat.*

The cryostat is simple in design: a large vacuum chamber enclosing a small

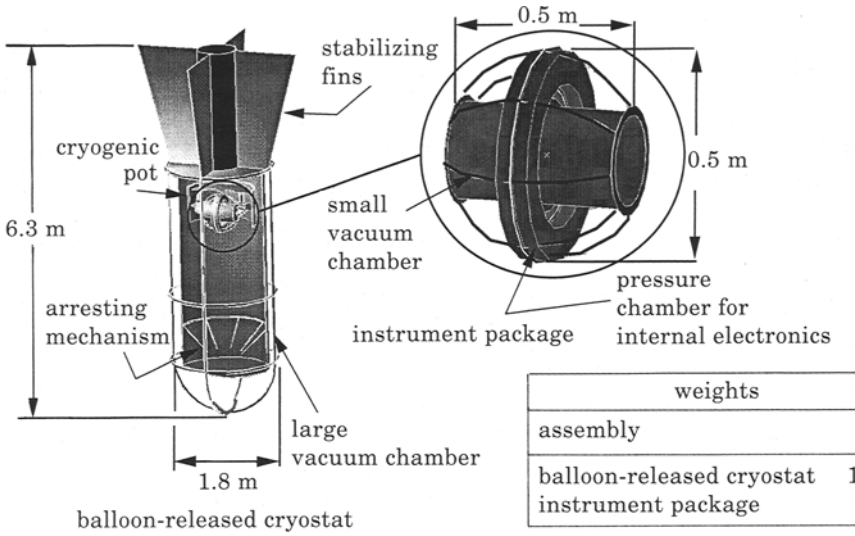


| weights | |
|---|---|
| assembly | kg |
| balloon-released cryostat | 1311 |
| instrument package | 30 |

Fig. 4. – Sketch of free-fall system and instrument package.

cryogenic container (pot) at the temperature of liquid nitrogen or liquid helium. There is no need to cool the entire vacuum chamber. During the up to 3 h ascent, the instrument package will sit in this container while it is rotated by the motor of the release mechanism (see fig. 4) to insure temperature uniformity. Once dropped, it falls into the relatively hot vacuum chamber; with radiation shielding on both the instrument package and the inside of the vacuum chamber, the temperature change within the instrument can be kept below 0.01 K during the 30 s free fall.

This approach allows the use of existing vacuum-chamber and cryogenic-container designs, and reduces the cost and especially the mass of the chamber over a fully cooled cryostat.

The instrument package is supported inside the cryogenic container and rotated during ascent at the signal frequency of 1 Hz through a spit arrangement. At release both support points of the spit are quickly withdrawn, leaving the package spinning about its axis at the desired signal frequency. This type of release system reduces the spurious components of the rotational velocity at release to a negligible level.

4) *Instrument package.*

The instrument package with a mass of 30 kg is virtually an autonomous system during the experimental period. It is in free fall within the vacuum chamber, relying only on internal power. Its only connection to the outside world is an infrared link to the on-board data system. Up to the point of release, the package relies on external power for heating and for operating its electronics.

The package consists of three sections: 1) small vacuum chamber; 2) pressure chamber; and 3) support structure thermal shield.

1) *Small vacuum chamber.* This vacuum chamber contains the detector and is held at $10^{-9}$ mbar for the liquid-nitrogen test and $10^{-11}$ mbar for the liquid-helium test, whereas the larger chamber in which it resides has a pressure of $10^{-6}$ mbar.

TABLE I. – *Mass budget.*

| Cryostat | kg | Instrument package | kg |
|---|---|---|---|
| large vacuum chamber | 732 | detector | 17 |
| holding frame | 350 | small vacuum chamber | 6 |
| spindle housing | 2 | pressure chamber | 2 |
| retraction plate | 1.56 | 2 detector cages | 1.4 |
| vacuum top flange | 29 | magnetic shield | 1 |
| cryogenic pot | 36 | batteries | 0.6 |
| parachute | 70 | compensation masses | 2 |
| 2 retraction motors | 6.4 | | |
| 4 tracks | 0.8 | Total instrument package | 30 |
| spin motor | 1 | | |
| external batteries | 57 | | |
| electronics | 25 | Gondola | kg |
| Total cryostat | 1311 | Total gondola | 161 |
| | | Grand total | 1502 |

A magnetic shield within the small vacuum chamber surrounds the detector to attenuate the effects of external magnetic fields on the instrument.

2) *Pressure chamber.* The pressure chamber is a toroidal vessel that is held at the waist of the small vacuum chamber (see fig. 4). Inside it are all the local electronics, batteries, and the piezoelectric accelerometers that are used to measure the instrument chamber's rotation rate with an estimated accuracy of 0.5°/s. The pressure chamber is held at an elevated pressure and temperature which permits the use of standard electronic components and batteries.

3) *Support structure.* The support structure, made of circular wires (see fig. 4), connects the pressure chamber to the smaller vacuum chamber and provides a support for the thermal radiation shield. Since the two chambers are at different temperatures, their connection is designed to reduce conduction between them while still maintaining a good structural tie.

A small conical trap, made from a wire net (see fig. 4), at the bottom of the large vacuum chamber captures the instrument package at the end of free fall. The instrument package will wedge itself into the trap and become more tightly bound with each bounce (parachute snap, etc.). Since the net is flexible, it further isolates the instrument chamber from impulse loads.

The preliminary mass budget of the free fall facility is shown in table I.

## 5. – Error budget.

Error sources are internal and external to the detector. The most important internal sources are: 1) amplifier noise; 2) thermal noise [17, 18]; and 3) viscous drag due to residual gas inside the condensers [19]. The most important external noise sources are: 1) the Earth's gravity gradient force and torque; 2) the Earth's

TABLE II. – *Error budget for the* WEP *test.*

| Noise source | Formula | Maximum differential $x$-acceleration | Frequency |
|---|---|---|---|
| amplifier noise | $\left(2T_A \frac{\omega_0^2}{\omega_S + \omega_P} \frac{k}{m_{eff}}\right)^{1/2}$ | $1 \cdot 10^{-14}\, g/\sqrt{\text{Hz}}$ | white |
| thermal noise ($LN_2$) $T = 77$ K, $Q = 15\,000$ | $\left(\frac{\omega_0 k}{m_{eff}} \frac{4T}{Q}\right)^{1/2}$ | $1.4 \cdot 10^{-13}\, g/\sqrt{\text{HZ}}$ | white |
| thermal noise (LHe) $T = 4$ K, $Q = 150\,000$ | $\left(\frac{\omega_0 k}{m_{eff}} \frac{4T}{Q}\right)^{1/2}$ | $1 \cdot 10^{-14}\, g/\sqrt{\text{HZ}}$ | white |
| cryostat's wall vibrations (wall velocity = 1 mm/s-$\sqrt{\text{Hz}}$) | $\frac{m}{m_{eff}} \chi a_{wall}$ | $5.6 \cdot 10^{-17}\, g/\sqrt{\text{HZ}}$ | white |
| residual gas in cryostat, ($p_{cryostat} = 10^{-6}$ mbar) | $\frac{m}{m_{eff}} \chi a_{gas}$ | $5 \cdot 10^{-17}\, g$ | $t_I^{-1}$ |
| Earth magnetic-field ferromagnetism | $f \frac{m}{l m_{eff}} \frac{\varepsilon \kappa_f B^2}{\varrho_f \mu_0}$ | $4 \cdot 10^{-15}\, g(LN_2)$<br>$4 \cdot 10^{-17}\, g(LHe)$ | $\omega_S$ |
| viscous drag | $\frac{pA}{m_{eff}} \frac{\dot{x}_m}{v_T}$ | $3 \cdot 10^{-15}\, g(LN_2)$<br>$3 \cdot 10^{-16}\, g(LHe)$ | $\omega_S$ |
| cryostat electrical-equipment ferromagnetism ($R = 0.5$ m) | $f \frac{m}{m_{eff}} \frac{\varepsilon \kappa_f B}{2 \varrho_f \mu_0} \frac{3 D_C}{R^4}$ | $3.5 \cdot 10^{-17}\, g(LN_2)$<br>$3.5 \cdot 10^{-19}\, g(LHe)$ | $\omega_S$ |
| Earth's gravity gradient force ($\delta x = 4\ \mu$m) | $\frac{m}{m_{eff}} \frac{2GM_E}{R^3} \delta x$ | $6.8 \cdot 10^{-13}\, g$ | $2\omega_S$ |
| Earth's gravity gradient torque ($\delta x = 4\ \mu$m) | $\frac{\Delta(J_x - J_z)}{l m_{eff}} \frac{2GM_E}{R^3}$ | $2.5 \cdot 10^{-13}\, g$ | $2\omega_S$ |
| other components | | $< 10^{-17}\, g$ | various |

magnetic-field interaction with the ferrous impurities in the sensing masses; and, similarly, 3) ferromagnetism related to the magnetic moment of the cryostat-fixed electrical equipment. The higher-mass moments produced by nearby masses non-corotating with the detector (*e.g.*, the vacuum chamber) need a more thorough evaluation which may lead to modifications of the detector geometry presented in this paper in order to make their error contribution to the differential acceleration negligible.

Table II provides a breakdown of the most important noise sources, their frequencies, and the relevant formulae. Symbols in table II are: $a_{gas}$ = drag deceleration from residual gas in cryostat = $10^{-12} g$; $a_{wall}$ = acceleration spectral density of cryostat's wall vibrations = $10^{-12}\, g/\sqrt{\text{Hz}}$ for wall vibrations of 1 mm/s-$\sqrt{\text{Hz}}$; $B$ = Earth's magnetic field at 40 km altitude and mid-latitudes = $4.5 \cdot 10^{-5}$ T; $D_C$ = cryostat-fixed magnetic-dipole moment = 1 A m$^2$; $k$ = Boltzman constant =

$= 1.38 \cdot 10^{-23}$ J/K; $Q$ = quality factor = 15 000 at $T = 77$ K and 150 000 at $T = 4$ K; $R$ = = distance of detector from source of disturbance; $T_A$ = amplifier's noise temperature = 10 mK; $v_T$ = thermal velocity of residual gas inside instrument package = 179 m/s; $\dot{x}_m$ = sensing-mass maximum velocity = $3.8 \cdot 10^{-3}$ m/s; $p$ = = pressure inside detector = $10^{-9}$ mbar for $T = 77$ K and $10^{-11}$ mbar for $T = 4$ K; $A$ = surface area of each sensing mass $\approx 0.012$ m$^2$; $\omega_0$ = detector resonant frequency = $20\pi$ rad/s (10 Hz); $\omega_S$ = signal frequency = $2\pi$ rad/s (1 Hz); $\omega_P$ = = frequency of pumping oscillator = $40\,000\pi$ rad/s (20 kHz); $\rho_f$ = density of iron = = 7800 kg/m$^3$; $\kappa_f$ = magnetic susceptivity per unit volume of iron (dimensionless, m.k.s.) = $2 \cdot 10^{-2}$ [20]; $\mu_0$ = magnetic permeability of vacuum = $4\pi \cdot 10^{-7}$ (m.k.s.); $f$ = = magnetic-shield attenuation factor = $10^{-4}$ for the test at $LN_2$ and $10^{-6}$ for the test at LHe; $\varepsilon$ = iron content in sensing masses $\approx 7 \cdot 10^{-3}$ for 6061 aluminum, and $\approx 10^{-5}$ for gold; $GM_E$ = Earth's gravitational constant = $3.986 \cdot 10^{14}$ m$^3$ s$^{-2}$; and $\Delta(J_x - J_z)$ = = difference between moments of inertia of sensing masses with geometrical error of 4 μm = $2.8 \cdot 10^{-7}$ kg m$^2$; $t_I$ = integration time = 30 s.

Noise components with frequencies well separated from the signal frequency $\omega_S$ do not affect the measurement so long as they do not drive the instrument off linearity for differential-mode perturbations or saturate the instrument for common-mode perturbations. These noise components will be filtered out of the output signal.

Preliminary tests on a prototype gradiometer (*i.e.* two accelerometers separated by a baseline of 50 cm in our case) at room temperature conducted at the Institute of Space Physics in Frascati, Italy have shown a sensitivity to differential accelerations of about $10^{-11}\, g/\sqrt{\text{Hz}}$ with a common-mode rejection factor of about 500. The sensitivity, in the absence of external disturbances, can be further improved by refrigerating the detector, increasing the masses of the sensing masses, and using better and yet available preamplifiers. Reduction of the external disturbances to a level smaller than $10^{-12} g$ can be obtained by means of the proposed free fall inside a shielding cryostat. Moreover, the reduction of the detector baseline from a finite length to zero reduces drastically the sensitivity to rotational accelerations and increases the common-mode rejection factor by improving the geometrical stability of the detector.

From our preliminary error analysis, it appears that the zero-baseline detector proposed in this paper will be capable of measuring the differential accelerations between the sensing masses with an accuracy of about $1.5 \cdot 10^{-13}\, g/\sqrt{\text{Hz}}$ in a 1 pico-$g$ environment at a temperature of 77 K, and $1.5 \cdot 10^{-14}\, g/\sqrt{\text{Hz}}$ at a temperature of 4 K. These differential acceleration accuracies correspond to a resolution, with 95% confidence level, of 5 parts in $10^{14}$ for $T = 77$ K and 5 parts in $10^{15}$ for $T = 4$ K in testing the weak-equivalence principle in a 30 s free fall.

## 6. – Features of differential acceleration detector.

A set of requirements that will yield the measurement accuracies indicated above are summarized in table III for the detector and in table IV for the free-fall system. Preliminary engineering analyses show that each of the indicated requirements is achievable with present technology. Several of the most important effects that influence these requirements are discussed below.

TABLE III. – *Detector requirements that will yield the desired accuracies.*

| Detector | Requirement |
|---|---|
| preamplifier noise temperature | $\leqslant 100$ mK |
| quality factor ($LN_2$) | $\geqslant 15\,000$ |
| quality factor (LHe) | $\geqslant 150\,000$ |
| sensing mass | $\geqslant 5.4$ kg |
| resonant frequency | $\leqslant 10$ Hz |
| common-mode rejection factor | $\leqslant 10^{-4}$ |
| linearity range | $\geqslant 10^6$ |
| pressure ($LN_2$) | $\leqslant 10^{-9}$ mbar |
| pressure (LHe) | $\leqslant 10^{-11}$ mbar |
| thermal gradient ($LN_2$) | $< 0.4$ K/m |
| thermal gradient (LHe) | $< 0.2$ K/m |

TABLE IV. – *Engineering requirements for free-fall facility that will yield desired accuracies.*

| Item | Requirement |
|---|---|
| *Instrument package* | |
| difference between maximum moment of inertia (MOI) and the other principal MOIs | 5% |
| offset between detector and instrument package centers of mass | $\leqslant 0.1$ mm |
| magnetic-dipole moment | $\leqslant 1$ A m$^2$ |
| magnetic attenuation factor ($LN_2$) | $\leqslant 10^{-4}$ |
| magnetic attenuation factor (LHe) | $\leqslant 10^{-6}$ |
| *Cryogenic pot* | |
| pressure | $< 10^{-6}$ mbar |
| temperature ($LN_2$) | 77 K |
| temperature (LHe) | 4 K |
| magnetic-dipole moment | $\leqslant 1$ A m$^2$ |
| *Release mechanism* | |
| overall rotational rate errors about any axis at instrument release | $< 6.3$ °/s |

i) *Common-mode rejection.*

An important parameter of a differential accelerometer is the common-mode rejection factor $\chi$. This factor expresses the attenuation of the effect of an external translational acceleration upon the instrument differential output. For example, an acceleration of $10^{-12}\,g$, with $\chi = 10^{-4}$, produces a differential output of only $10^{-16}\,g$.

The common-mode rejection factor depends on the closeness to equality of the resonant frequencies and quality factors of the two sensing masses and on the geometrical stability of the detector. A common-mode response differs from a differential-mode response (*i.e.* the response to a WEP violation) because in the former case the two sensing masses move in phase, while in the latter case they move in opposition. With the accuracy allowed by machining tolerances and inhomogeneities of materials, a common-mode rejection factor of about $10^{-4}$ should be achievable.

ii) *Gravity gradient torques and forces.*

Thanks to the cylindrical symmetry of the sensing masses' ellipsoids of inertia, the 2nd-order gravity gradient torques (*i.e.* those associated with the quadrupole mass moment) about the longitudinal axis $y$ (see fig. 3) are equal to zero for perfectly homogeneous masses with an exact symmetry. In a real situation machining imperfections and material inhomogeneities account for small departures from perfect cylindrical symmetry and hence produce non-null 2nd-order gravity gradient torques. The machining errors for similar condenser probes previously built are less than 0.5 μm. Inhomogeneities of the aluminum alloy can contribute an error of several μm [21] and are therefore more important than the machining errors. A common-mode rejection factor of $10^{-4}$ requires a maximum offset along the instrument $z$-axis (see fig. 3) between the centers of mass (CsM) of the sensing masses no greater 4 μm. This value implies a careful selection of the aluminum ingot. The ingot must be: *a*) preheated in order to reduce microsegregation and *b*) carved out of the center part of a larger ingot in order to keep the macrosegregation below the tolerable level (*i.e.* the variation of Cu and other heavy elements across the thickness of the ingot should be less than 0.03%). Moreover, with an offset of 4 μm, either the gravity gradient torques or forces produce a differential acceleration error four orders of magnitude smaller than the upper bound of the detector's linearity range. This is conservative because, thanks to the frequency separation provided by the instrument rotation, the gravity-related disturbances are only required to be within the instrument linearity range.

The cryostat shell also generates a gravity gradient inside the cryostat. Its strength, however, is negligible with respect to the Earth's gravity gradient (for the formulae see ref. [22]).

iii) *Pressure and thermal gradient.*

A limit on the tolerable pressure difference $\Delta p$ inside the instrument package can be obtained by requiring that the acceleration $a = A\,\Delta p/m_{\text{eff}}$ produced by the air piston effect (d.c. signal) on the surface $A$ of each sensing mass [19] be at least three orders of magnitude smaller than the upper bound of the differential acceleration linearity limit. Consequently, for $A \approx 0.012\,\text{m}^2$ and $m_{\text{eff}} = 9.8\,\text{kg}$, the tolerable pressure difference should be less than $10^{-7}\,\text{Pa}$ for the test at $LN_2$ and less than $10^{-8}\,\text{Pa}$ for the test at LHe. However, the maximum tolerable pressure is also related to the maximum allowable thermal gradient through the radiometer effect, *i.e.* the acceleration produced by gas molecules emitted from regions with different temperatures [19]. This effect is likely to produce an acceleration error modulated at the signal frequency because, as the instrument package rotates, it faces regions of the large vacuum chamber at different temperatures. The acceleration produced by the radiometer effect is $a = p(\Delta T/\Delta x)/(2\varrho T)$ [19] where $p$ is the pressure, $T$ the temperature and $\varrho$ the density of the sensing mass. For $\varrho = 2700\,\text{kg/m}^3$ (aluminum), $p = 10^{-7}\,\text{Pa}$ ($10^{-9}\,\text{mbar}$), and $T = 77\,\text{K}$ ($LN_2$) the equation above implies that a thermal gradient of 0.4 K/m is required for an acceleration error equal to $10^{-14}\,g$. At a temperature of 4 K (LHe), a pressure of $10^{-9}\,\text{Pa}$ ($10^{-11}\,\text{mbar}$) is required for an acceleration error of $10^{-15}\,g$ and a temperature gradient of 0.2 K/m, which is comparable to the value required for $T = 77\,\text{K}$.

A thermal gradient across the detector also affects the resonant frequencies of the sensing masses through variations of: Young's modulus of the material, the geometry

of the torsional springs, and the moments of inertia of the sensing masses. Consequently, a thermal gradient changes differentially the resonance frequencies of the sensing masses and ultimately affects the common-mode rejection factor.

The common-mode rejection factor is related to the temperature variation $\Delta T$ across the detector as follows: $\chi \approx |\alpha + \alpha_E| \Delta T$, where $\alpha$ is the thermal-expansion coefficient and $\alpha_E$ the thermal coefficient of Young's modulus. For aluminum at low temperatures $\alpha \ll \alpha_E$, $\alpha_E \sim -3.5 \cdot 10^{-4}\,K^{-1}$[23], while $\chi$ is required to be $\leq 10^{-4}$. Consequently, the tolerable temperature gradient for a 0.5 m long detector must be smaller than 0.6 K/m for either $T = 77$ K or $T = 4$ K. This value is consistent with the upper-bound values for the thermal gradient dictated by the radiometer effect.

iv) *Magnetic disturbances.*

Magnetic shielding around the detector is primarily required for abating magnetic torques and forces acting on the ferromagnetic impurities in the materials of the sensing masses. The ferromagnetic impurities (permanent magnetic dipoles) interact with the magnetic field inside the cryostat (Earth's field and electrical-equipment fields) to produce mechanical torques and forces acting on the sensing masses[3].

The most critical magnetic-related accelerations are at the signal frequency, like those generated by the interaction of the ferromagnetic impurities of the rotating sensing mass with a non-corotating magnetic field like the Earth's or the cryostat-fixed magnetic field.

Requirements of magnetic cleanliness must be imposed on the electrical equipment on the cryostat. If the magnetic-dipole moment of the electrical equipment is no greater than 1 A m$^2$, the related effects are reduced to a negligible level.

The most severe magnetic disturbance is produced by the torque from the Earth's magnetic field acting on ferromagnetic impurities of aluminum (gold has an iron content less than $10^{-3}$%[24]). For the $\sim$ 0.7% ferrous impurities[25] in the 6061 aluminum, a magnetic-shielding factor of $10^{-4}$ and degaussing of the detector are required for reducing the magnetic-related acceleration to about $10^{-15}\,g$ for the test at the $LN_2$ temperature. A magnetic-shielding factor of $10^{-4}$ can be obtained with a few layers of $\mu$-metal placed around the detector. A the LHe temperature, a blanket of superconducting material (*e.g.*, lead) provides a magnetic-shielding factor better than $10^{-6}$ and, consequently, produces an acceleration error of the order of $10^{-17}\,g$.

v) *Instrument package dynamics.*

The instrument rotates around the center of mass (CM) of the entire instrument package which ideally coincides with the CsM of the two sensing masses. However, if the various CsM are not exactly on the plane perpendicular to the sensitive axis $x$, centrifugal forces will have a non-null (d.c.) component along the $x$-axis proportional to the offset $\delta d_x$, along the same axis. Consequently, the offset $\delta d_x$, between the CM of the instrument package and the CsM of the sensing masses, must be less than 0.1 mm for a condenser gap of 60 $\mu$m and a spin frequency of 1 Hz in order for the instrument response to remain well within the dynamic range. The 0.1 mm upper limit on the $\delta d_x$ offset can be met via a careful construction and subsequent balancing of the instrument package.

Since the principal moments of inertia of the instrument package will not be equal, a precession of the spin axis will ensue if its initial orientation is not aligned with the axis of maximum moment of inertia. The precession frequency is well separated from

the signal frequency and hence filterable if we require that the maximum moment of inertia (aligned with the spin axis) be 5% greater than either of the two other principal moments of inertia. This difference provides gyroscopic stability and a precession frequency of 0.05 Hz, *i.e.* twenty times lower than the signal frequency of 1 Hz.

The design of the instrument package is such as to provide an ellipsoid of inertia close to spherical. Moreover, the magnitude and orientation of its principal moments of inertia will be fine-tuned (on the ground) by means of a set of small compensation masses. Some of the compensation masses of the set will be utilized to place the CM of the instrument package within 0.1 mm of the sensing masses CsM.

The amplitude of precession must also be limited in order not to reduce significantly the signal strength because of large precession amplitudes. The precession amplitude will be less than 1° if the angular-velocity components perpendicular to the spin axis at release are less than $0.0175\,\omega_S$, *i.e.* less than 6.3°/s for a rotation frequency of 1 Hz. Typical rotation rates measured on the gondola of a 40 km high balloon are ~ 0.01°/s about the horizontal axes and less than 1°/s about the vertical axis [26].

## 7. – Conclusions.

The vertical free fall inside a cryostat dropped from a high-altitude balloon of a high-sensitivity differential acceleration detector could make possible a test of the weak-equivalence principle to an accuracy, with 95% confidence level, of 5 parts in $10^{14}$ at the temperature of liquid nitrogen and 5 parts in $10^{15}$ at the temperature of liquid helium in a 30 s integration time. Consequently, the accuracy in validating the weak-equivalence principle could be improved by a few orders of magnitude with respect to the most accurate tests conducted thus far.

Since this test will be conducted in free fall, it will also provided experience valuable for a more ambitious space emission.

## REFERENCES

[1] R. v. EÖTVÖS: *Math. Naturw. Ber. Ungarn*, 8, 65 (1890).
[2] R. v. EÖTVÖS, V. PEKAR and E. FETEKE: *Ann. Phys. (Leipzig)*, **68**, 11 (1922).
[3] P. G. ROLL, R. KROTKOV and R. H. DICKE: *Ann. Phys. (N. Y.)*, **26**, 442 (1964).
[4] V. B. BRAGINSKY and V. I. PANOV: *Sov. Phys. JETP*, **34**, 463 (1972).
[5] I. I. SHAPIRO, C. C. COUNSELMAN and R. W. KING: *Phys. Rev. Lett.*, **36**, 555 (1976).
[6] J. G. WILLIAMS *et al.*: *Phys. Rev. Lett.*, **36**, 551 (1976).
[7] I. I. SHAPIRO: *Solar systems tests of general relativity: recent results and present plans*, in *Proceedings of GR-12*, edited by N. ASHBY and D. BARLETT (Cambridge University Press, Cambridge, 1990).
[8] C. W. F. EVERITT: *Progr. Astron. Aeron.*, **108**, 898, AIAA (1986).
[9] F. FULIGNI and V. IAFOLLA: *Fifth force measurements from a free falling platform at balloon altitudes*, in *Proceedings of the Sixth Marcel Grossman Meeting on General Relativity, Kyoto, Japan, 1991*, edited by H. SATO and T. NAKAMURA (World Scientific, Singapore, 1992), p. 1325.
[10] I. CIUFOLINI, F. FULIGNI, V. IAFOLLA and S. NOZZOLI: *Nuopvo Cimento C*, **15**, 973 (1992).

[11] E. C. LORENZINI, M. L. COSMO, M. D. GROSSI and T. ROTHMAN: *A method for testing the principle of equivalence with improved accuracy*, Smithsonian Astrophysical Observatory, Technical Note TP91-001 (Cambridge, Mass., 1991).
[12] E. C. LORENZINI, F. FULGINI, J. B. ZIELINSKI, M. L. COSMO, M. D. GROSSI, V. IAFOLLA and T. ROTHMAN: *Adv. Space Res.*, **14**, 113, 118 (1994).
[13] R. E. HALPERN: *Prog. Astron. Aeron.*, **108**, 1, AIAA (1986).
[14] F. BORDONI, F. FULIGNI and V. IAFOLLA: *Nuovo Cimento C*, **13**, 49 (1990).
[15] M. D. GROSSI *et al.*: *Experimental Testing of Corpuscular Radiation Detectors*, Raytheon Final Report, DARPA Contract F49620-87-C-0050 (Newport, R.I., 1989).
[16] E. C. LORENZINI, G. G. GULLAHORN and F. FULGINI: *J. Appl. Phys.*, **63**, 216 (1988).
[17] V. B. BRAGINSKY and A. B. MANUKIN: *Measurement of Weak Forces in Physics Experiments* (The University of Chicago Press, Chicago, Ill., 1974), p. 7.
[18] R. P. GIFFARD: *Phys. Rev. D*, **14**, 2478 (1976).
[19] P. W. WORDEN jr., C. W. F. EVERITT and M. BYE: *Satellite Test of the Equivalence Principle*, Stanford University Report (Palo Alto, Cal., 1990).
[20] R. M. BOZORTH: *Ferromagnetism* (Van Nostrand, 1961).
[21] NATIONAL BUREAU OF STANDARDS: *Macrosegregation in Wrought Aluminum Alloys, Processing/Microstructure/Property Relationships in 2024 Aluminum Alloy Plates*, NBS Report 83-2669 (1983).
[22] E. R. MAPOLES: *Development of a Superconducting Gravity Gradiometer for a Test of the Inverse Square Law*, PhD Thesis, Stanford University (Palo Alto, Cal., 1981).
[23] F. J. LAVOIE (Editor): *Materials Engineering: Materials Selector 1987* (Penton Publication, 1986), p. 72.
[24] JOHNSON MATTHEY COMPANY: private communication (1992).
[25] THE ALUMINUM ASSOCIATION: *Registration Record of Aluminum Association Designations and Chemical Composition Limits for Wrought Aluminum and Wrought Aluminum Alloys* (Washington, D.C., 1993).
[26] G. NYSTROM *et al.*: *Design of a lightweight stabilized balloon gondola for X-ray observations*, in *Proceedings of the Symposium on Thirty Years of Scientific Ballooning in India* (Tata Institute of Fundamental Research, Hyderabad, 1992).